Spatial and Seasonal Variation of Biomineral Suspended Particulate Matter Properties in High-Turbid Nearshore and Low-Turbid Offshore Zones

Michael Fettweis [1] and Byung Joon Lee [2,*]

[1] Operational Directorate Natural Environment, Royal Belgian Institute of Natural Sciences, Gulledelle 100, B-1200 Brussels, Belgium; mfettweis@naturalsciences.be

[2] Department of Disaster Prevention and Environmental Engineering, Kyungpook National University, 2559 Gyeongsang-daero, Sangju, Gyeongbuk 742-711, Korea

[*] Correspondence: bjlee@knu.ac.kr; Tel.: +82-54-530-1444

Abstract: Suspended particulate matter (SPM) is abundant and essential in marine and coastal waters, and comprises a wide variety of biomineral particles, which are practically grouped into organic biomass and inorganic sediments. Such biomass and sediments interact with each other and build large biomineral aggregates via flocculation, therefore controlling the fate and transport of SPM in marine and coastal waters. Despite its importance, flocculation mediated by biomass-sediment interactions is not fully understood. Thus, the aim of this research was to explain biologically mediated flocculation and SPM dynamics in different locations and seasons in marine and coastal waters. Field measurement campaigns followed by physical and biochemical analyses had been carried out from 2004 to 2011 in the Belgian coastal area to investigate bio-mediated flocculation and SPM dynamics. Although SPM had the same mineralogical composition, it encountered different fates in the turbidity maximum zone (TMZ) and in the offshore zone (OSZ), regarding bio-mediated flocculation. SPM in the TMZ built sediment-enriched, dense, and settleable biomineral aggregates, whereas SPM in the OSZ composed biomass-enriched, less dense, and less settleable marine snow. Biological proliferation, such as an algal bloom, was also found to facilitate SPM in building biomass-enriched marine snow, even in the TMZ. In short, bio-mediated flocculation and SPM dynamics varied spatially and seasonally, owing to biomass-sediment interactions and bio-mediated flocculation.

Keywords: suspended particulate matter; aggregates; flocculation; biomass; sediment

1. Introduction

Suspended particulate matter (SPM), produced by biological and geophysical actions on the Earth's crust, enters into marine and coastal waters and is dispersed by flow-driven transportation, such as advection and dispersion [1–3]. The SPM concentration is an important parameter to understand the marine ecosystem as it controls the water turbidity and mediates many physical and biochemical processes [4–6].

SPM comprises a wide variety of biomineral clay to sand sized particles, comprising living (microbes, phyto- and zooplankton) and non-living organic matter (fecal and pseudo-fecal pellets, detritus and its decomposed products from microbial activity such as mucus, exopolymers), and minerals from a physico-chemical (e.g., clay minerals, quartz, feldspar) and biogenic origin (e.g., calcite, aragonite, opal), which are practically grouped into organic biomass and inorganic sediments [7]. It is important to note that when clays or other charged particles and polymers are in suspension, they become attached to each other and form fragile structures or flocs with compositions, sizes, densities,

and structural complexities that vary as a function of turbulence and biochemical composition [3,8–11]. Flocculation combines biomass and sediments into larger aggregates (i.e., flocs) that can be classified as either mineral, biomineral, or biological aggregates. Flocculation usually integrates aggregation and disaggregation (i.e., breakup) kinetics, depending on the hydrodynamics of a suspension. Electrostatic and colloidal chemistry is the fundamental driver for flocculation in a cohesive suspension. For example, high ionic strength reduces the electrostatic repulsion between colloidal particles, thereby increasing the aggregation of colloidal suspension. Also, regarding the heterogeneity of a natural suspension with various biomass and sediments, physical and biochemical conditions are favorable for flocculation, like low turbulence intensity, high ionic strength, and sticky polymeric substances, which help individual biomineral particles to build large aggregates. Clay mineralogy is also important for determining electrochemistry and flocculation capability. Depending on the biomass composition, such aggregates are classified into mineral, biomineral, and biological aggregates [12,13]. Mineral and biomineral aggregates form in the sediment-enriched environment, such as a turbidity maximum zone (TMZ) or a nearshore area [6,14,15], while biological aggregates (i.e., marine snow) form in the mineral-depleted environment typically found in an offshore zone (OSZ) [16].

Flocculation mediated by biological composition determines the size, density, and settling velocity of aggregates [12,14,17]. For example, in a tidal cycle, low flow intensity during slack water enhances flocculation capability, building large, settleable aggregates, whereas high flow intensity at peak flow reduces flocculation capability, breaking down aggregates to small, less (or hardly) settleable aggregates or primary particles [5,18]. Moreover, sticky biomass (e.g., extracellular polymeric substances (EPSs) or transparent extracellular polymers (TEPs)) helps build large biomineral aggregates [7,19–22]. Flocculation which can be mediated by biological factors consequently controls sedimentation, resuspension, deposition, and erosion, and determines the overall SPM dynamics in marine and coastal waters [12,23].

Bio-medicated flocculation and SPM dynamics are important in science and engineering because they eventually control the sediment, carbonaceous, and nitrogenous mass balances at the regional or global scale [24,25]. Despite their importance, bio-mediated flocculation and SPM dynamics are not fully understood in coastal and marine waters. Geologists and hydraulic engineers have focused more on sediments and less on biomass [3,14], and marine biologists vice versa [16]. In our opinion, the biomass-sediment interactions in coastal and marine waters have only recently been studied in a systematic and quantitative way [7,9,13,26–29], and mathematical models which can take into account the heterogeneous composition/morphology of biomineral aggregates were developed only a few years ago [12,30]. These efforts should be paid more attention.

Therefore, the aim of the study was to add to our current understanding of bio-mediated flocculation and its impact on the SPM in marine and coastal waters. First, we investigated the spatial variation of SPM dynamics in a sediment-enriched TMZ and a mineral-depleted OSZ, especially concerning bio-mediated flocculation. Second, we investigated the seasonal variation of SPM dynamics in a TMZ to understand how seasonal changes in biological activity, especially algae blooms, affect bio-mediated flocculation and SPM dynamics. This paper describes and discusses bio-mediated flocculation and SPM dynamics for different locations and seasons.

2. Materials and Methods

2.1. Site Description

The study area is situated in the Southern Bight of the North Sea, specifically in the Belgian coastal zone. Measurements have indicated SPM concentrations of 20–70 mg/L in the nearshore area; reaching 100 to more than a few g/L near the bed; lower values (<10 mg/L) occur in the offshore [31]. As shown in Figure 1, the MOW1 measurement site is located in the TMZ. The Gootebank (G-Bank), Hinderbank (H-Bank), and Kwintebank (K-Bank) sites are in the OSZ, out of or at the edge of the turbidity maximum. Satellite images of surface SPM and chlorophyll-a (Chl) concentrations in the

study area show clear spatial and seasonal changes. Regarding the seasonality, the annual cycle of
SPM concentration in the high turbidity area off the Belgian coast is mainly caused by the seasonal
biological cycle, rather than wind and waves. Wind strengths and wave heights have a seasonal signal,
but these do not explain the large differences observed in SPM concentration [31,32]. This seasonality
is linked with the seasonal changes in aggregate size and thus settling velocity due to biological effects.
The aggregate sizes and settling velocities are smaller in winter and larger in summer. As a result, the
SPM is more concentrated in the near-bed layer, whereas in winter, the SPM is better mixed throughout
the water column. This explains the inverse correlation found between the surface SPM and the Chl
concentrations in Figure 1. Water depths of the measuring area vary between 5 and 35 m. The mean
tidal ranges at Zeebrugge are 4.3 and 2.8 m at spring and neap tides, respectively. The tidal current
ellipses are elongated in the nearshore area and become gradually more semicircular towards the
offshore area. The current velocities near Zeebrugge (nearshore) vary from 0.2 to 1.5 m/s during
spring tide and from 0.2 to 1.0 m/s during neap tide. Salinity varies between 28 and 34 practical
salinity units (PSU) in the coastal zone, because of the wind-induced advection of water masses and
river discharge [33,34]. The most important sources of SPM are from the erosion and resuspension of
the Holocene mud deposits outcropping in the Belgian nearshore area; the French rivers discharging
into the English Channel, and the coastal erosion of the Cretaceous cliffs at Cap Gris-Nez and Cap
Blanc-Nez (France) are only minor sources [35,36].
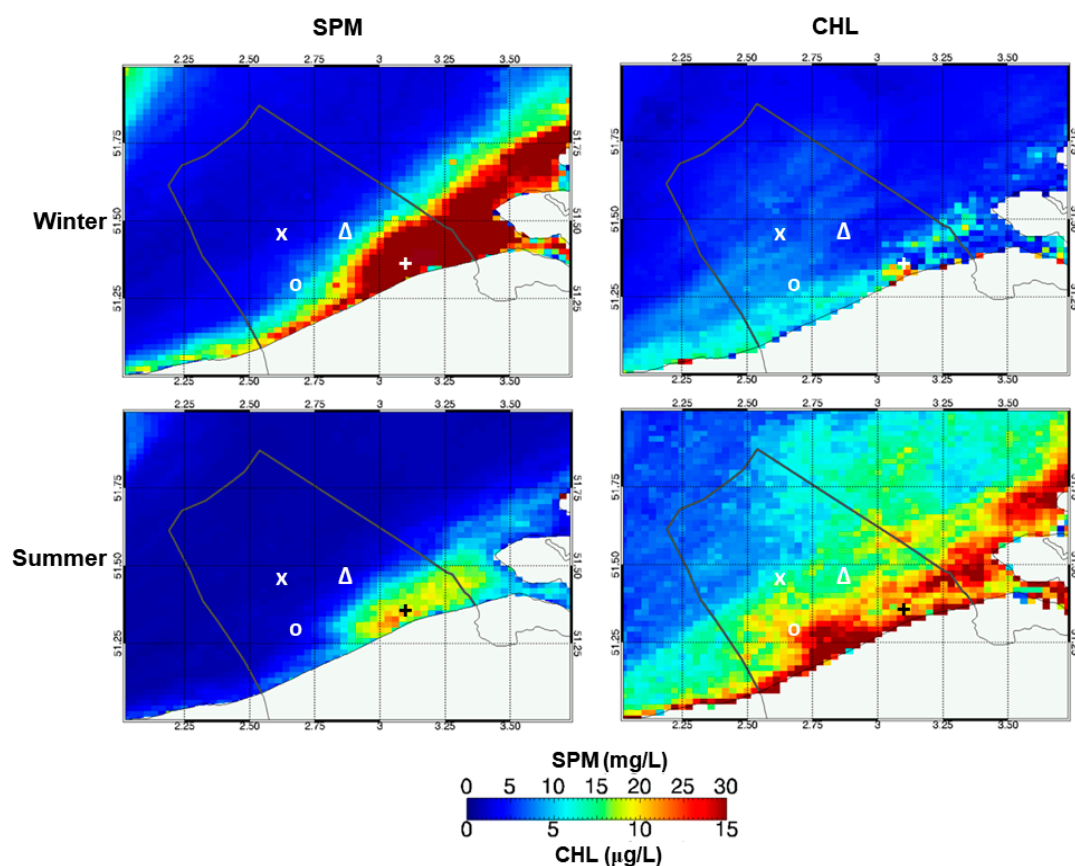
Figure 1. Mean surface suspended particulate matter (SPM) and chlorophyll-a (CHL) concentrations in
the southern North Sea during the winter (October–March, top) and summer season (April–September,
bottom) derived from the MERIS satellite. The +, Δ, X, and O symbols indicate the measurement
sites of MOW1, Gootebank (G-Bank), Hilnderbank (H-Bank), and Kwintebank (K-Bank), respectively.
Turbidity maximum zone (TMZ) has SPM concentrations above 15–20 mg/L and the offshore zone
(OSZ) below 10 mg/L.

2.2. Tidal Measurements

Field measurements in the TMZ (MOW1) and in the OSZ (G-Bank, H-Bank, and K-Bank) were carried out about four times a year from February 2004 until 2011. During each campaign, sensor measurements (flow, SPM dynamics) and water sampling (SPM properties) were executed, while the research vessel was moored to maintain a specific measuring position for a 13-h tidal cycle. A Sea-Bird SBE09 SCTD carousel sampling system (containing twelve 10 L Niskin bottles) (Sea-Bird Electronics Inc., Bellevue, WA, USA) was kept at least 4.5 m below the surface and about 3 m above the bottom. A LISST 100X (Laser In-Situ Scattering and Transmissometry, range 2.5–500 µm) (Sequoia Scientific Inc., Bellevue, WA, USA) was attached directly to the carousel sampling system to measure particle size distribution (PSD) at the same location as the water sampling system [37]. The volume concentration of each size group was estimated with an empirical volume calibration constant, which was obtained under a presumed sphericity of particles [37–39]. The LISST has a sampling volume which permits it to statistically sample the less numerous large aggregates, but it cannot detect aggregates larger than 500 µm or smaller than 2.5 µm. Particles smaller than the size range affect the entire PSD, with an increase in the volume concentration of the smallest two size classes, a decrease in the next size classes and, an increase in the largest size classes [40]. Similar remarks have been formulated by Graham and coworkers [41], who observed an overestimation of one or two orders of magnitude in the number of fine particles measured by the LISST. A rising tail in the lowest size classes of the LISST occurs regularly in the data during highly turbulent conditions and is interpreted as an indication of the presence of very fine particles and thus a break-up of the aggregates. Particles exceeding the LISST size range of 500 µm also contaminate the PSD. The large out of range particles increase the volume concentration of particles in multiple size classes in the range between 250 and 500 µm and in the smaller size classes [42–44]. The occurrence of rising tail in the largest size classes indicates the occurrence of large particles rather than an absolute value. Other uncertainties of the LISST-100C are related to the often non-spherical shape of the particles occurring in nature [40,41,44]. A hull mounted, acoustic Doppler current profiler (ADCP) type, Workhorse Mariner 300 kHz (RD Instruments, Poway, CA, USA), was used to determine the velocity profiles.

2.3. Water Samples and Analysis

A Niskin bottle of the carousel sampling system was closed every 20 min, thus collecting about 40 samples during a 13 h flood-ebb tidal cycle. Note that the carousel sampling system was deployed to take water samples in the middle of the water column, at least 3 m above the bed layer. The carousel was brought aboard every hour. Three sub-samples from each water sample were then filtered on board using pre-weighed filter papers (Whatman GF/C, Sigma-Aldrich, St. Louis, MO, USA). In total, 120 filtrations were thus carried out per tidal cycle. After filtration, the filter papers were rinsed with demineralized water ($\pm$50 mL) to remove the salt, dried at 105 °C, and weighed again to determine the SPM concentrations. Every hour, a fourth sub-sample was filtered on board to determine particulate organic carbon (POC) and particulate organic nitrogen (PON) concentrations. The residues on the filter paper were carefully collected and acidified with 1 N HCl. Then, the POC and PON of the residues were quantified with a Carbon Nitrogen elemental analysis.

2.4. Grain Size and Mineralogical Analysis

Primary grain size and mineralogical analyses were performed to determine the mineralogical composition of the SPM samples. Suspension samples were obtained by the centrifugation of seawater collected by an ALFA Laval MMB 304S flow-through centrifuge (Alfa Laval Corp., Lund, Sweden), while the bed samples have been taken with a Van Veen grab sampler. Collected and stored samples were dried at 105 °C and chemically treated by adding HCl and H_2O_2 in order to remove the organic and carbonate fractions. The pretreated samples were rinsed with demineralized water, dried at 105 °C, and added to 100 mL demineralized water with 5 mL of peptizing agent (a mixture of

NaCO$_3$ and Na-oxalate). The suspension was dispersed and disaggregated using a magnetic stirrer and an ultrasonic bath. The grain size distribution and clay-silt-sand fractions of the SPM sample were analyzed with a Sedigraph 5100 (Micrometrics Instrument Corp., Norcross, GA, USA) for the fraction < 75 μm and sieved for the coarser fraction. The mineralogical composition of the clay fraction of the samples was determined with a Seifert 3003 theta-theta X-ray diffractometer (GE Measurement & Control, Billerica, MA, USA). Details of the analytical methods are documented in the earlier dissertation [36].

3. Results and Discussion

3.1. Mineralogical Characteristics of TMZ and OSZ

The mineralogical composition of the bed materials in the TMZ and OSZ are shown in Table 1. The respective clay and quartz contents of the bed materials in the TMZ were 25.0% and 39.6%, respectively, whereas those in the OSZ were 12.4% and 66.7%. Thus, the bed materials in the TMZ were found to be a mud-sand mixture, while the bed materials in the OSZ were sandy. Carbonates, such as calcite, Mg-calcite, aragonite, and dolomite, comprise about 20% and 10% of the TMZ and OSZ, respectively. Feldspar (i.e., K-feldspar and plagioclase) was also found to be an important content of the bed materials of the TMZ and OSZ, with a value of about 8%. Amorphous species in the TMZ and OSZ comprised 4.2% and 1.1%, respectively. Amorphous species are considered biogenic minerals influenced by biogeochemical actions [36,45]. The clay minerals at both sites comprised about 5% Kaolinite, 10% Chlorite, and 85% 2:1 layered silicates.

Table 1. Average mineralogical fractions (%) of the bulk deposits and suspended particulate matters (SPM) in the turbidity maximum zone (TMZ) and offshore zone (OSZ) measuring sites.

Material	Location	Clays	Quartz	Carbonates	Amorphous	Feldspar	Others
Bed Materials	TMZ	25.0	39.6	21.1	4.2	8.0	2.1
	OSZ	12.4	66.7	10.7	1.1	8.1	0.9
SPM	TMZ	36.2	14.6	29.9	12.7	4.2	2.3
	OSZ	31.3	20.6	29.7	10.1	6.4	1.8

In contrast to the bed materials, the SPM in the TMZ and OSZ had a similar mineralogical composition. For instance, the clays and quartz contents of the SPM only differed by 5% between the TMZ and OSZ, and the contents of carbonates, amorphous, feldspar, and others differed by less than 2.5%. This happened because the SPM samples do not contain coarser bed material, as the sand grains in suspension are seldom found above the near-bed layer. This also shows that the SPM in the TMZ and OSZ has the same origin, as suggested by the earlier geological survey in this area [35,36]. It is also important to note that the respective fractions of carbonate and amorphous species are large, at about 30% and 11% for both the TMZ and OSZ, thereby indicating high biological activity in the measuring area.

3.2. Spatial Variation of SPM Dynamics in the TMZ and OSZ

During the entire measurement period (2004–2011), the POC/SPM ratios in the OSZ were substantially higher than those in the TMZ (Figure 2a). This observation indicates that the SPM in the OSZ comprises more biomass and less sediments, and vice versa for the SPM in the TMZ. A scatter plot with POC content and SPM concentration shows the transition from a high mineral to the low-mineral SPM, when shifting from the TMZ to the OSZ (Figure 3). Generally, POC content increased with a decreasing SPM concentration (i.e., mineral-depleted condition). The mineral-depleted SPM in the OSZ seemed analogous to the muddy marine snow from an Australian coastal area where minerals were bound together with planktonic and transparent exopolymer particulate matter [46]. However,

the PON/POC ratios of the TMZ and OSZ did not show such a clear difference during the entire study period, and their 95% confidence levels overlapped (Figure 2b).
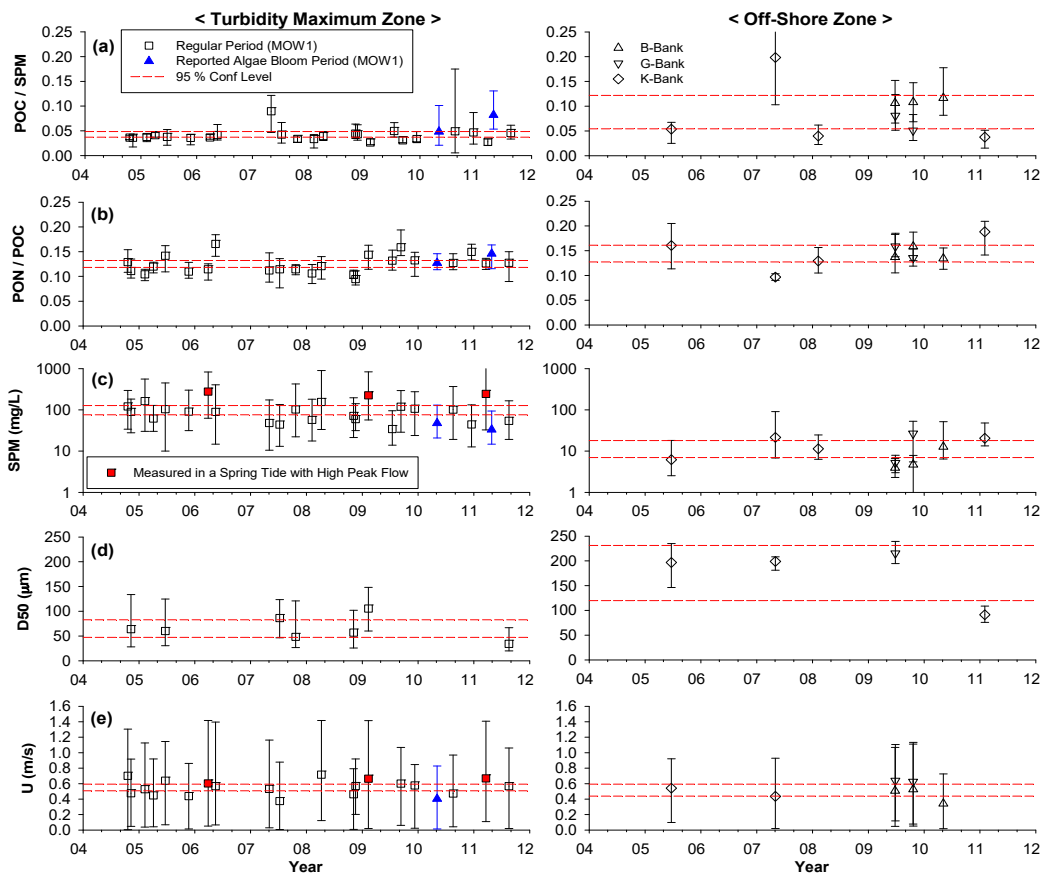
Figure 2. Spatial and seasonal variation of experimental indices in the measurement sites, during the entire measurement period, from 2004 to 2011. The left and right panels illustrate the data obtained from the turbidity maximum zone (TMZ) and the offshore zone (OSZ), respectively. (**a**) POC content in the SPM; (**b**) POC/PON ratio; (**c**) SPM concentration; (**d**) D50: median of the volumetric particle/aggregate size distribution; (**e**) U: flow velocity; MOW1: measurement site in the TMZ; B-Bank, G-Bank, and K-Bank: measurement sites in the OSZ.
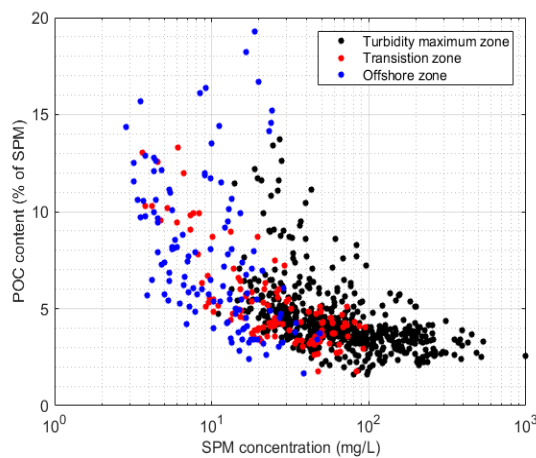

Figure 3. Scatter plot of POC content (% of SPM) versus SPM concentration. The coupled data sets of POC content and SPM concentration were obtained from all the 13 h measurement campaigns.

SPM concentrations in the TMZ are about an order magnitude higher than those in the OSZ (Figure 2c), similar to the satellite images of SPM concentration in Figure 1. This observation suggests that a substantial amount of sediment resides in the TMZ, which is transported back and forth in the flood and ebb tides. In addition, SPM concentrations in the TMZ were more vulnerable to flow intensity. High flow velocity (U) was found to increase SPM concentrations (e.g., 29 March 2006, 7 February 2008, 10 February 2009 and 21 March 2011, in Figure 2), because it increases sediment erosion and resuspension from the sea floor. It is also important to note that the TMZ had a two to three times smaller aggregate size (D50; median of the volumetric particle/aggregate size distribution) than the OSZ (Figure 2d) [15]. Thus, the TMZ enriched with sediments (i.e., higher SPM concentration and lower POC/SPM) had a lower flocculation capability (i.e., lower D50) than the OSZ. Tang and Maggi reported that small, dense aggregates are formed in sediment(mineral)-enriched environments, such as the TMZ in this study, whereas large, fluffy aggregates are formed in biomass-enriched environments [13,29]. The former was defined as mineral or biomineral aggregates, and the latter as biological aggregates.

SPM and POC concentrations and D50 in the TMZ were subject to ups and downs during the 13-h tidal cycle (Figure 4a). Generally, SPM and POC concentrations increased to their maximum around the peak flows. Biomass and minerals were likely combined in large, settleable biomineral aggregates, because SPM and POC concentrations had the same up-and-down movement during a tidal cycle. Such biomineral aggregates in the TMZ are vulnerable to aggregation and disaggregation (i.e., breakup), depending on the flow intensity (turbulence), available aggregation time to reach the equilibrium aggregate size, and organic matter content, therefore changing D50 in a flow-varying tidal cycle [5,18]. D50 increased to the maximum when approaching slack water, but decreased to a minimum around peak flow. Regarding flocculation kinetics, aggregation kinetics dominated over disaggregation kinetics for the slack water, and vice versa for the peak flow [5,18]. In contrast, SPM and POC concentrations and D50 in the OSZ were rather constant, randomly scattered without apparent ups and downs (Figure 4b), showing that aggregation kinetics dominate over disaggregation kinetics for the entire period. SPM in the OSZ might be mainly composed of biomass and some mineral particles, building more shear-resistant and less settleable marine snow [46]. Although biological aggregates (i.e., marine snow) are usually much larger, up to several millimeters, than mineral or biomineral aggregates, they settle more slowly because of their low density and fluffy structure [30]. The latter is confirmed by an earlier study [38], where the excess density of aggregates has been calculated for some of the tidal cycles investigated here; the mean excess density was 550 kg/m^3 and the mean D50 of the aggregates 65 μm (five tidal cycles) in the TMZ versus 180 kg/m^3 and 115 μm (three tidal cycles) in the OSZ. Although both the TMZ and the OSZ are governed by tidal dynamics, small differences in the current regime occur between both areas [15], as is also shown in Figure 4. The TMZ is situated in the nearshore, where the current ellipses are more elongated, whereas more offshore, the ellipses tend to be more spherical. This will cause higher velocity gradients, stronger turbulence, more stress exerted on the aggregates, and a reduction of the time needed for the aggregates to reach equilibrium size in the TMZ. Considering these differences in hydrodynamics, the mineral and biomineral aggregates in the TMZ are more susceptible to the hydrodynamics than the biological aggregates in the OSZ.

Time series of the PSDs during the 13 h tidal cycles are shown in Figure 5, for the TMZ and OSZ, respectively. PSDs in the TMZ skewed toward a smaller size around peak flow (e.g., t = 3, 4 h at location MOW1 on 10 July 2007) and then to a larger size around slack water (e.g., t = 6, 7 h). Except for the PSDs in 23 October 2007, the other PSDs in the TMZ showed bimodality, comprising microflocs (20–200 μm) and macroflocs (>200 μm), as reported in the earlier studies [5]. The primary peak of microflocs in a PSD was prominent around the peak flow. However, while approaching the slack water, the secondary peak of macroflocs became dominant over the primary peak. Low flow/turbulence intensity might promote the aggregation of microflocs (i.e., mineral, biomineral aggregates) to macroflocs (i.e., biological aggregates) [4,5,18]. On the other hand, large hardly-settleable biological aggregates

which were suspended in the water column might dominate in the slack water. Maggi and Tang recently reported that larger biological aggregates can be lighter and even settle slower than smaller mineral, bio-mineral aggregates [13]. Here, larger biological aggregates can be suspended in the slack water, while smaller mineral, bio-mineral aggregates settle and deposit, thereby developing the secondary peak of biological aggregates.
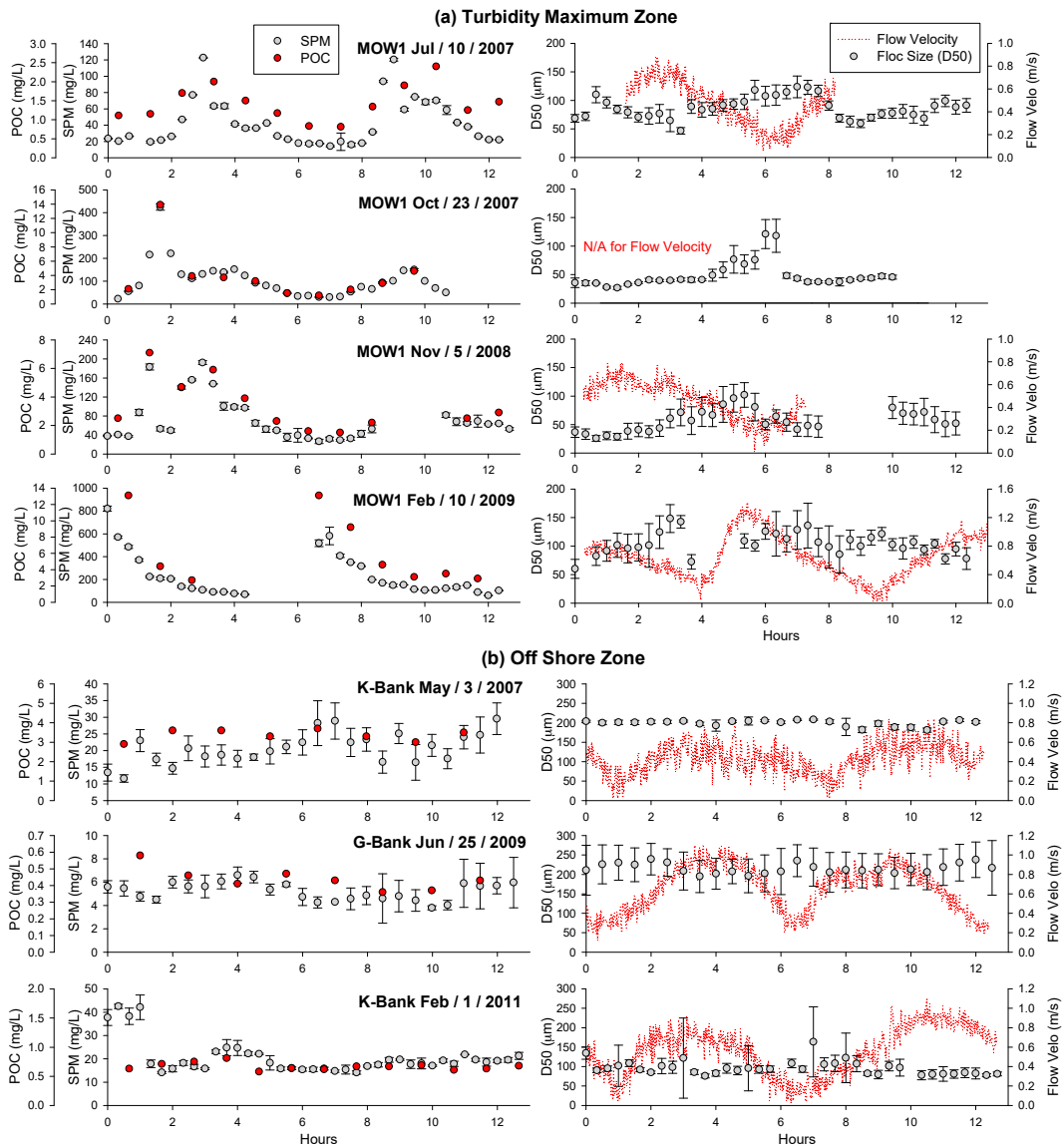
Figure 4. Dynamic behaviors of suspended particulate matter (SPM) and particulate organic carbon (POC) concentrations and aggregate size (D50) in 13-h tidal cycles, in (**a**) the turbidity maximum zone (TMZ) and (**b**) the offshore zone (OSZ). Each set of the SPM/POC and D50 data was measured on a specific date of a field campaign. MOW1: measurement site in the TMZ; K-Bank and G-Bank: measurement sites in the OSZ.

However, PSDs in the OSZ remained rather constant during the entire tidal cycle, consistently skewing toward a larger size (Figure 5b). A substantial fraction of the PSDs occupied the upper most measuring bin of the LISST-100X instrument (i.e., 500 μm). Aggregates in the OSZ, even with such a large size, apparently did not properly settle but floated in the water column (see also the previous paragraph and Figure 4). Thus, SPM in the OSZ is likely composed of large but light, fluffy, and hardly-settleable biological aggregates (i.e., marine snow), whereas SPM in the

TMZ comprises dense, compact, and readily-setteable mineral, biomineral aggregates, as well as biological aggregates [13,29,30,46]. However, note that this argument is supported by a rather indirect measurement of SPM dynamics in this research and observations from earlier studies. Direct ways of measuring aggregate morphology might be required in the future to explain realistic structures and behaviors of mineral, biomineral, and biological aggregates.
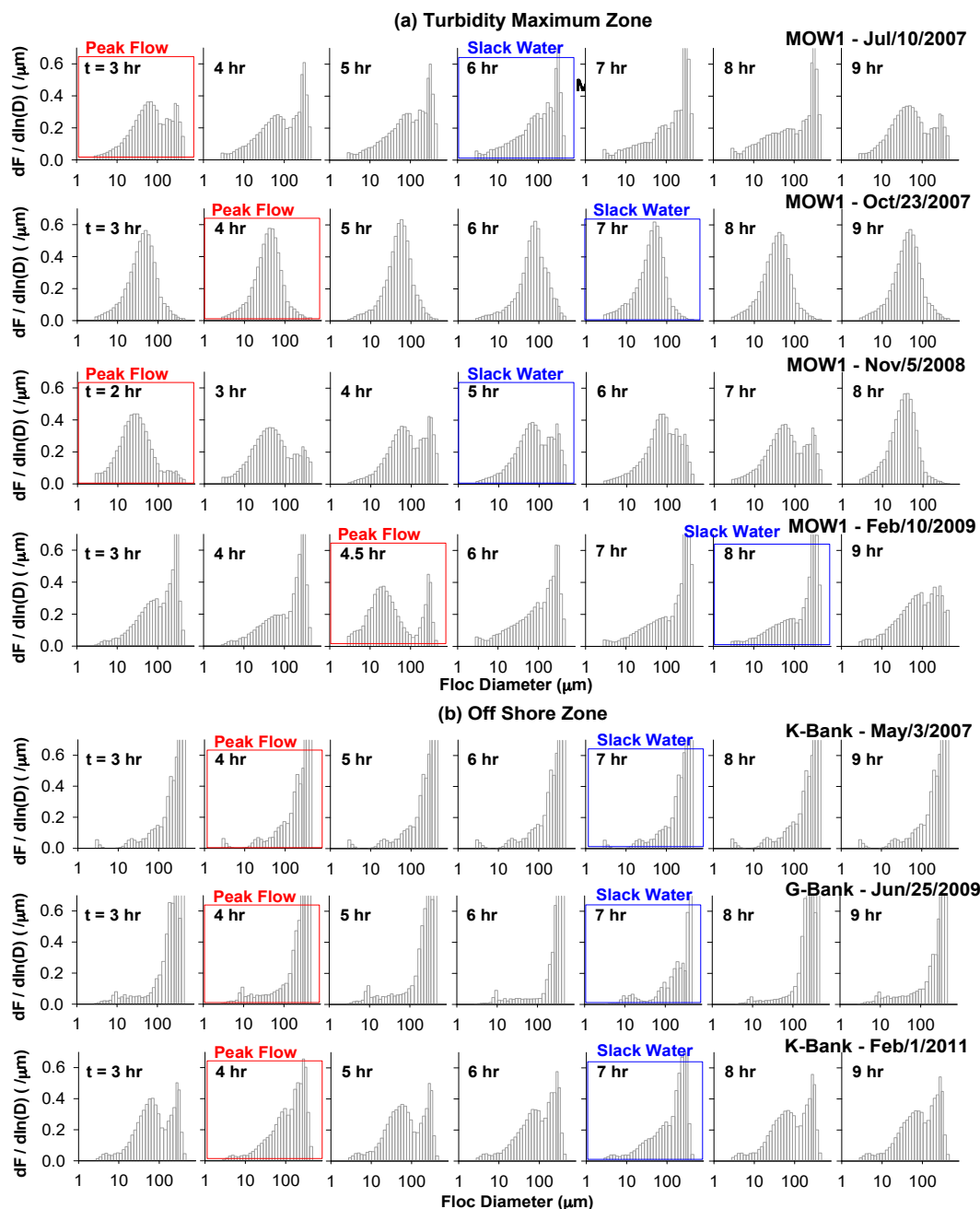
Figure 5. Particle size distributions (PSDs) of suspended particulate matter (SPM) in 13-h tidal cycles, for (**a**) the turbidity maximum zone (TMZ) (MOW1) and (**b**) the offshore zone (OSZ) (K-Bank and G-Bank). Each set of the PSDs was measured on a specific date of a field campaign. Each PSD was plotted on a logarithmic scale, and the fraction of a size bin was normalized by the width of the size bin in y-axis. Thus, dF/dln (D) is the normalized volumetric fraction by the width of the size interval in the log scale, in accordance with the lognormal distribution function [5,47].

### 3.3. SPM Dynamics during the Algae Bloom and Normal Periods in the TMZ

Flow intensity of the spring and neap tides was found to alter SPM properties (e.g., aggregate size and settling velocity) and SPM dynamics (e.g., flocculation, sedimentation, and deposition) in the TMZ (i.e., the MOW1 site). A spring tide, associated with a strong peak flow (up to 1.5 m/s), increased SPM concentrations substantially, compared to a neap tide with a weak peak flow (up to 1.0 m/s). For example, SPM concentrations increased up to 800 mg/L during a spring tide (e.g., MOW1—10 February 2009 in Figure 4a), whereas they remained under 120 mg/L during a neap tide (e.g., MOW1—10 July 2007). When the pairs of the maximum SPM concentration (SPM$_{max}$) and peak flow velocity (U$_{max}$) in each 13-h tidal cycle are plotted (Figure 6), they are proportional. A spring tide with high U$_{max}$ resulted in high SPM$_{max}$, because it enhanced the disaggregation, erosion, and resuspension of sediment particles/aggregates. However, a neap tide with low U$_{max}$ resulted in low SPM$_{max}$, because it enhanced aggregation, sedimentation, and deposition. Thus, the fate and transport of SPM in the TMZ, which was governed by aggregation-disaggregation, sedimentation-resuspension, and erosion-deposition, highly depended on flow intensity. However, an exception against the SPM-flow intensity relation was found during an algae bloom period.
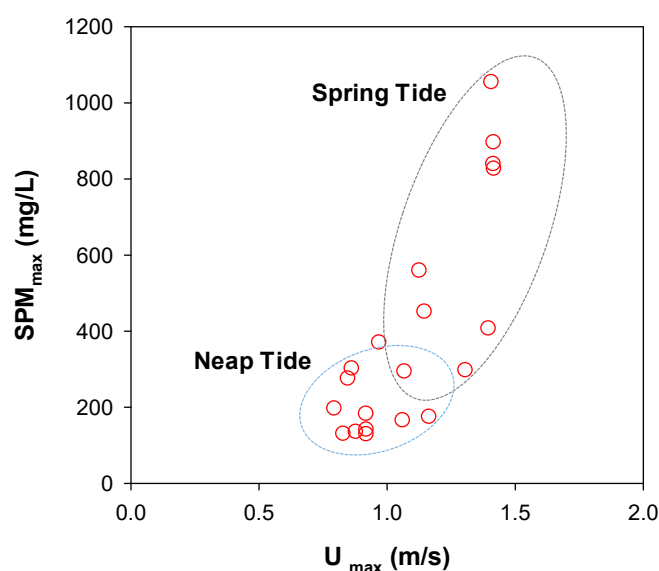

Figure 6. Plots of maximum suspended particulate matter concentration (SPMmax) versus maximum flow velocity (Umax). SPM concentration and flow velocity were measured in the middle of the water column. Each point represents a pair of SPMmax and Umax measured in a 13-h tidal cycle. All the data were measured in the turbidity maximum zone (TMZ) from 2004 to 2011.

During the reported spring algae bloom (MOW1—26 April 2011 in Figure 7a), SPM and POC concentrations did not show a clear up-and-down trend with tide, but behaved similar to those in the OSZ. The aggregate sizes during the algae bloom period (26 April 2011 in Figure 7a) were two to three times larger than aggregates during the normal period, measured at the same site four months later (18 August 2011 in Figure 7b). Although aggregates were enlarged (>100 μm) during the algae bloom period, they did not show a clear sign of downward settling. Considering that such large aggregates during the algae bloom period were subject to floatation without a clear sign of sedimentation and resuspension, they were found to be lighter and less settleable than during a regular period, and thus more similar to the marine snow (i.e., biological aggregates) found in the OSZ (see Section 3.2). In the TMZ, two different aggregates may thus occur: (1) sediment-enriched, dense, and settleable biomineral aggregates during normal periods; and (2) biomass-enriched, light, and less settleable marine snow during algal bloom periods (Figure 8). The latter type of aggregate corresponds better to the one observed in the OSZ. The aggregates occurring during algae bloom periods or in the OSZ have a lower

settling velocity as a larger fraction is composed of organic matter and sticky bio-polymers organized in a fluffy structure [16,48].
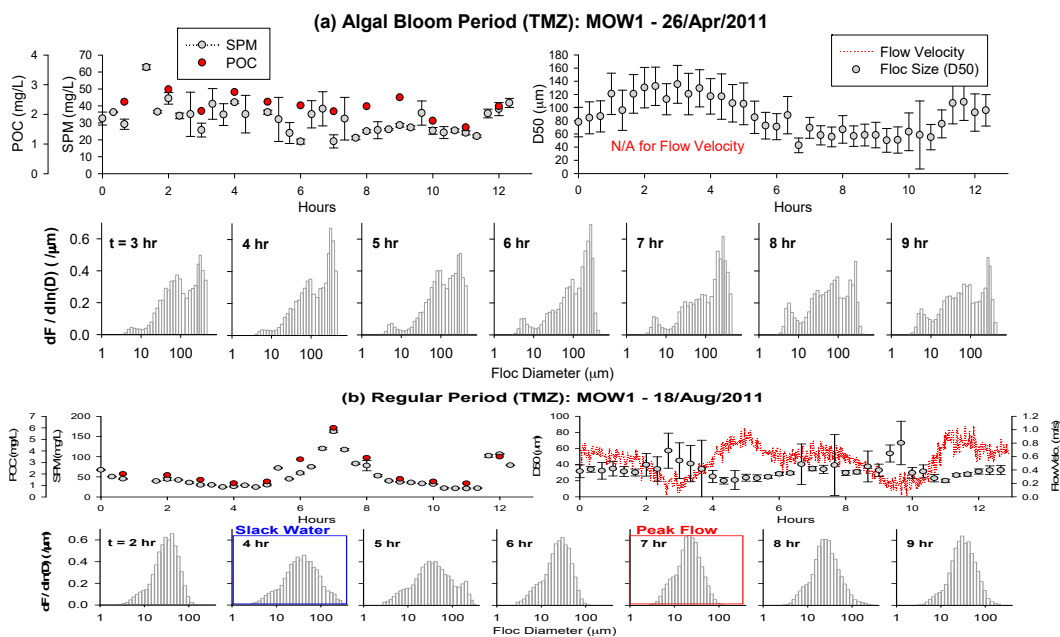
Figure 7. Dynamic behaviors of suspended particulate matter (SPM) and particulate organic carbon (POC) concentrations, aggregate size (D50), and particle size distribution (PSD) in a 13-h tidal cycle. The two data sets were collected in the TMZ (i.e., the MOW1 site) on different dates in 2011, representing (**a**) algal bloom period and (**b**) regular periods.
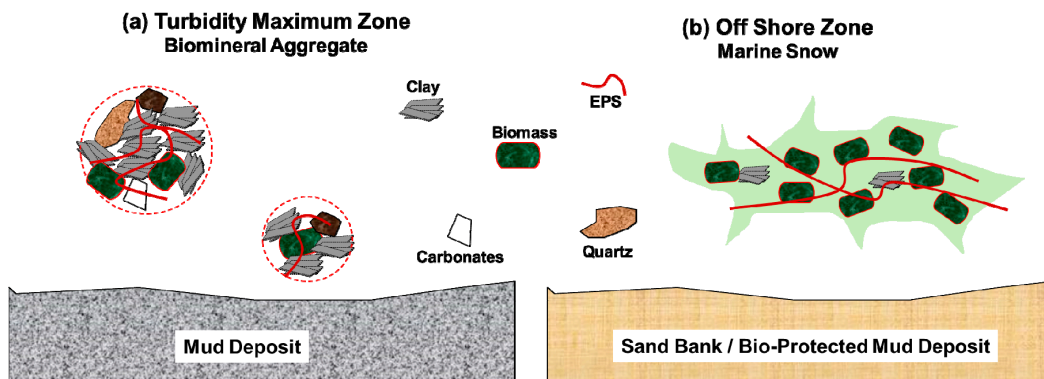
Figure 8. Schematic diagrams of (**a**) biomineral aggregates in the turbidity maximum zone (TMZ) and (**b**) biological marine snow in the offshore zone (OSZ). EPS: extracellular polymeric substances.

Previous studies, carried out in the same TMZ, reported that large and settleable biomineral aggregates were dominant SPM species during bio-enriched spring and summer periods [31,32]. These large, settleable biomineral aggregates are contrary to less settleable biological aggregates observed in this current study. However, it is important to note that the SPM samples in this study were taken in the middle of the water column, well above the near-bed layer. Dense, compacted, and settleable biomineral aggregates might be stored in the near-bed layer, causing mineral-depletion in the water column, and hence less dense, fluffy, and hardly settleable biological aggregates might be formed and float around in the water column. Enhanced primary production during an algal bloom period generates more sticky, particle-binding polymeric substances, such as EPSs and TEPs. These sticky polymeric substances can not only enhance flocculation, but also reduce the erosion and resuspension

of muddy deposits from the seabed to the water column [49]. A large amount of cohesive sediments are thus stored in or on the seafloor as a fluid-mud layer or a muddy deposit, and the marine snow with more biomass and less sediments is suspended in the water column [3]. This SPM behavior during an algal bloom period with high primary production agrees with the satellite images of low SPM and high Chl concentrations in summer (Figure 1). Similar observations were made in the port of Zeebrugge. High primary production and low turbulence in summer provoked a large amount of mud deposition in the near-bed layer (or formation of a fluid mud layer) and reduction of the SPM concentration in the water column.

Reviewing other studies [28,50] revealed similar SPM dynamics around an algal bloom period. Proliferation of a specific algae group could enhance flocculation and store sediments in the near-bed layer, and hence could cause large but suspended biological aggregates and a low SPM concentration in the water column. Maerz and co-workers [51] have been looking at the whole gradient from the nearshore TMZ to the OSZ; they have found a maximum settling velocity in the transition zone between the TMZ and the OSZ where the aggregates are larger as compared to near-coast TMZ and denser as compared to the low turbid OSZ. This maximum in settling velocity is caused by similar gradients in aggregate size, POC content, density, and chlorophyll concentration than found in our data. The fact that algae are involved in these observed gradients points to seasonal influences. Another study [52], however, does not confirm the leading role of the algae bloom on SPM dynamics. The reason for these different findings may be due to differences in, amongst others, hydrodynamics, wave climate, nutrient availability, and algae species at the different study sites. The importance of each of these parameters will explain to a smaller or larger part the observed seasonal variations in SPM dynamics.

Biomineral and biological aggregates are often approximated by a single parameter (e.g., a characteristic diameter) in practical applications, although they are very different in composition and mechanical property. For example, a traditional aggregate structure model, based on fractal theory, includes only mineral particles and disregards organic matter, which is instead assumed to be part of the pore space for simplicity and ease [53,54]. This approximation might not be valid for biological aggregates (i.e., marine snow) with a high content of organic matter or in environments where aggregate properties change in time (regular versus algae bloom period) or space (inside and outside harbours). Thus, the heterogeneity of aggregates, at least the two fractions of biomass and sediments, should be considered when developing a rigorous aggregate structure model and accurately predicting the fate and transport of biomass and sediments in marine and coastal waters [30].

A higher biomass content (indicated by a higher POC/SPM ratio) was generally found to enhance flocculation, thereby increasing aggregate size. However, the quantity of biomass is not the only factor determining the flocculation capability. For example, in June 2009 at G-Bank (Figure 2a), aggregate size increased to over 200 μm, even with a low POC/SPM. Besides the quantity of biomass, the quality, such as stickiness, is important for controlling flocculation kinetics, as reported in previous research [50,55]. Specifically, extracellular polymeric substances (EPSs) or transparent extracellular polymers (TEPs) are sticky and increase flocculation [19,20,22,23]. Long polymeric chain structures of EPSs and TEPs, which are produced by aquatic microorganisms (e.g., algae), can bind biomass and sediment particles to large mineral, biomineral, and biological aggregates. Even in an unfavorable chemical condition for flocculation (e.g., terrestrial water with low ionic strength), a small amount of EPSs and TEPs can cause substantial flocculation, because they can overcome the electrostatic repulsive force of negatively-charged colloidal particles and bind such particles to large aggregates [56,57]. Therefore, qualitative measures of biomass, such as EPS and/or TEP concentration, likely need to be included to explain bio-mediated flocculation and SPM dynamics in marine and coastal waters.

4. Conclusions

The monitoring and analysis of SPM dynamics explained how organic biomass and inorganic sediment interact with each other to build large biomineral aggregates or marine snow in marine and coastal waters. SPM in the TMZ and OSZ had a similar mineralogical composition, but encountered

different fates in association with biomass. SPM in the TMZ built sediment-enriched, dense, and settleable biomineral aggregates, whereas SPM in the OSZ was composed of biomass-enriched, light, and less settleable marine snow. Biological proliferation, such as an algae bloom, also facilitated the occurrence of marine snow in the water column, even in the TMZ. Enhanced flocculation in summer could also scavenge SPM in the water column down to the sea bed, resulting in a low SPM concentration in the water column. In short, bio-mediated flocculation and SPM dynamics were found to vary spatially and seasonally, affected by the biota. The proposed concept to combine organic and mineral particles in aggregates will help us to better understand and predict bio-mediated flocculation and SPM dynamics in marine and coastal waters.

Author Contributions: M.F. conceived, designed, and performed the experiments; B.J.L. analyzed the experimental data; and M.F. and B.J.L. wrote the paper.

Conflicts of Interest: The authors declare no conflict of interest.

References

1. Ouillon, S.; Douillet, P.; Andrefouet, S. Coupling satellite data with in situ measurements and numerical modeling to study fine suspended-sediment transport: A study for the lagoon of New Caledonia. *Coral Reefs* **2004**, *23*, 109–122.

2. Perianez, R. Modelling the transport of suspended particulate matter by the Rhone River plume (France). Implications for pollutant dispersion. *Environ. Pollut.* **2005**, *133*, 351–364. [CrossRef] [PubMed]

3. Winterwerp, J.; van Kesteren, W. *Introduction to the Physics of Cohesive Sediment in the Marine Environment*; Elsevier B.V.: Amsterdam, The Netherlands, 2004.

4. Lee, B.J.; Toorman, E.; Molz, F.J.; Wang, J. A two-class population balance equation yielding bimodal flocculation of marine or estuarine sediments. *Water Res.* **2011**, *45*, 2131–2145. [CrossRef] [PubMed]

5. Lee, B.J.; Fettweis, M.; Toorman, E.; Molz, F.J. Multimodality of a particle size distribution of cohesive suspended particulate matters in a coastal zone. *J. Geophys. Res. Oceans* **2012**, *117*, C03014. [CrossRef]

6. Chen, M.S.; Wartel, S.; Temmerman, S. Seasonal variation of floc characteristics on tidal flats, the Scheldt estuary. *Hydrobiologia* **2005**, *540*, 181–195. [CrossRef]

7. Droppo, I.G. Rethinking what constitutes suspended sediment. *Hydrol. Process.* **2001**, *15*, 1551–1564. [CrossRef]

8. Eisma, D. Flocculation and de-flocculation of suspended matter in estuaries. *Neth. J. Sea Res.* **1986**, *20*, 183–199. [CrossRef]

9. Droppo, I.; Leppard, G.; Liss, S.; Milligan, T. *Flocculation in Natural and Engineered Environmental Systems*; CRC Press Inc.: Boca Raton, FL, USA, 2005.

10. Jago, C.F.; Kennaway, G.M.; Novarino, G.; Jones, S.E. Size and settling velocity of suspended flocs during a phaeocystis bloom in the tidally stirred Irish Sea, NW European Shelf. *Mar. Ecol. Prog. Ser.* **2007**, *345*, 51–61. [CrossRef]

11. Tan, X.L.; Zhang, G.P.; Yi, H.; Reed, A.H.; Furukawa, Y. Characterization of particle size and settling velocity of cohesive sediments affected by a neutral exopolymer. *Int. J. Sediment Res.* **2012**, *27*, 473–485. [CrossRef]

12. Maggi, F. Biological flocculation of suspended particles in nutrient-rich aqueous ecosystems. *J. Hydrol.* **2009**, *376*, 116–125. [CrossRef]

13. Maggi, F.; Tang, F.H.M. Analysis of the effect of organic matter content on the architecture and sinking of sediment aggregates. *Mar. Geol.* **2015**, *363*, 102–111. [CrossRef]

14. Van Leussen, W. Estuarine Macroflocs: Their Role in Fine-Grained Sediment Transport. Ph.D. Thesis, Utrecht University, Utrecht, The Netherlands, February 1994.

15. Fettweis, M.; Francken, F.; Pison, V.; Van den Eynde, D. Suspended particulate matter dynamics and aggregate sizes in a high turbidity area. *Mar. Geol.* **2006**, *235*, 63–74. [CrossRef]

16. Alldredge, A.; Silver, M. Characteristics, dynamics and significance of marine snow. *Prog. Oceanogr.* **1988**, *20*, 41–82. [CrossRef]

17. Markussen, T.N.; Andersen, T.J. A simple method for calculating in situ floc settling velocities based on effective density functions. *Mar. Geol.* **2013**, *344*, 10–18. [CrossRef]

18. Lee, B.J.; Toorman, E.; Fettweis, M. Multimodal particle size distributions of fine-grained sediments: Mathematical modeling and field investigation. *Ocean Dyn.* **2014**, *64*, 429–441. [CrossRef]

19. Passow, U. Transparent exopolymer particles (TEP) in aquatic environments. *Prog. Oceanogr.* **2002**, *55*, 287–333. [CrossRef]

20. Engel, A.; Thoms, S.; Riebesell, U.; Rochelle-Newall, E.; Zondervan, I. Polysaccharide aggregation as a potential sink of marine dissolved organic carbon. *Nature* **2004**, *428*, 929–932. [CrossRef] [PubMed]

21. Sahoo, G.B.; Nover, D.; Schladow, S.G.; Reuter, J.E.; Jassby, D. Development of updated algorithms to define particle dynamics in Lake Tahoe (CA-NV) USA for total maximum daily load. *Water Resour. Res.* **2013**, *49*, 7627–7643. [CrossRef]

22. Mari, X.; Passow, U.; Migon, C.; Burd, A.; Legendre, L. Transparent Exopolymer Particles: Effects on carbon cycling in the ocean. *Prog. Oceanogr.* **2017**, *151*, 13–37. [CrossRef]

23. Jouon, A.; Ouillon, S.; Douillet, P.; Lefebvre, J.P.; Fernandez, J.M.; Mari, X.; Froidefond, J. Spatio-temporal variability in suspended particulate matter concentration and the role of aggregation on size distribution in a coral reef lagoon. *Mar. Geol.* **2008**, *256*, 36–48. [CrossRef]

24. Tranvik, L.J.; Downing, J.A.; Cotner, J.B.; Loiselle, S.A.; Striegl, R.G.; Ballarore, T.J.; Dillon, P.; Finlay, K.; Fortino, K.; Knoll, L.B.; et al. Lakes and reservoirs as regulators of carbon cycling and climate. *Limnol. Oceanogr.* **2009**, *54*, 2298–2314. [CrossRef]

25. Gudasz, C.; Bastviken, D.; Premke, K.; Steger, K.; Tranvik, L.J. Constrained microbial processing of allochthonous organic carbon in boreal lake sediments. *Limnol. Oceanogr.* **2012**, *57*, 163–175. [CrossRef]

26. Barkmann, W.; Schafer-Neth, C.; Balzer, W. Modelling aggregate formation and sedimentation of organic and mineral particles. *J. Mar. Syst.* **2010**, *82*, 81–95. [CrossRef]

27. Burd, A.; Jackson, G. Modeling steady-state particle size spectra. *Environ. Sci. Technol.* **2002**, *36*, 323–327. [CrossRef] [PubMed]

28. De Lucas Pardo, M.A.; Sarpe, D.; Winterwerp, J.C. Effect of algae on flocculation of suspended bed sediments in a large shallow lake. Consequences for ecology and sediment transport processes. *Ocean Dyn.* **2015**, *65*, 889–903. [CrossRef]

29. Tang, F.H.M.; Maggi, F. A mesocosm experiment of suspended particulate matter dynamics in nutrient- and biomass-affected waters. *Water Res.* **2016**, *89*, 76–86. [CrossRef] [PubMed]

30. Maggi, F. The settling velocity of mineral, biomineral, and biological particles and aggregates in water. *J. Geophys. Res. Oceans* **2013**, *118*, 2118–2132. [CrossRef]

31. Fettweis, M.; Baeye, M.; Van der Zande, D.; Van den Eynde, D.; Lee, B.J. Seasonality of floc strength in the southern North Sea. *J. Geophys. Res. Oceans* **2014**, *119*, 1911–1926. [CrossRef]

32. Fettweis, M.; Baeye, M. Seasonal variation in concentration, size and settling velocity of muddy marine flocs in the benthic boundary layer. *J. Geophys. Res. Oceans* **2015**, *120*, 5648–5667. [CrossRef]

33. Fettweis, M.; Francken, F.; Van den Eynde, D.; Verwaest, T.; Janssens, J.; Van Lancker, V. Storm influence on SPM concentrations in a coastal turbidity maximum area with high anthropogenic impact (southern North Sea). *Cont. Shelf Res.* **2010**, *30*, 1417–1427. [CrossRef]

34. Lacroix, G.; Ruddick, K.; Ozer, J.; Lancelot, C. Modelling the impact of the Scheldt and Rhine/Meuse plumes on the salinity distribution in Belgian waters (southern North Sea). *J. Sea Res.* **2004**, *52*, 149–163. [CrossRef]

35. Fettweis, M.; Nechad, B.; Van den Eynde, D. An estimate of the suspended particulate matter (SPM) transport in the southern North Sea using SeaWiFS images, in situ measurements and numerical model results. *Cont. Shelf Res.* **2007**, *27*, 1568–1583. [CrossRef]

36. Zeelmaekers, E. Computerized Qualitative and Quantitative Clay Minerology: Introduction and Application to Known Geological Cases. Ph.D. Thesis, Katholieke Universiteit Leuven, Leuven, Belgium, April 2011.

37. Agrawal, Y.; Pottsmith, H. Instruments for particle size and settling velocity observations in sediment transport. *Mar. Geol.* **2000**, *168*, 89–114. [CrossRef]

38. Fettweis, M. Uncertainty of excess density and settling velocity of mud flocs derived from in situ measurements. *Estuar. Coast. Shelf Sci.* **2008**, *78*, 426–436. [CrossRef]

39. Mikkelsen, O.; Curran, K.; Hill, P.; Milligan, T. Entropy analysis of in situ particle size spectra. *Estuar. Coast. Shelf Sci.* **2007**, *72*, 615–625. [CrossRef]

40. Andrews, S.; Nover, D.; Schladow, S. Using laser diffraction data to obtain accurate particle size distributions: The role of particle composition. *Limnol. Oceanogr. Methods* **2010**, *8*, 507–526. [CrossRef]

41. Graham, G.W.; Davies, E.; Nimmo-Smith, A.; Bowers, D.G.; Braithwaite, K.M. Interpreting LISST-100X measurements of particles with complex shape using digital in-line holography. *J. Geophys. Res. Oceans* **2012**, *117*, C05034. [CrossRef]

42. Mikkelsen, O.A.; Hill, P.S.; Milligan, T.; Chant, R.J. In situ particle size distributions and volume concentrations from a LISST-100 laser particle sizer and a digital floc camera. *Cont. Shelf Res.* **2005**, *25*, 1959–1978. [CrossRef]

43. Smith, S.J.; Friedrichs, C.T. Size and settling velocities of cohesive flocs and suspended sediment aggregates in a trailing suction hopper dredge plume. *Cont. Shelf Res.* **2011**, *31*, S50–S63. [CrossRef]

44. Davies, E.; Nimmo-Smith, A.; Agrawal, Y.; Souza, A. LISST-100 response to large particles. *Mar. Geol.* **2012**, *307–311*, 117–122. [CrossRef]

45. Kastner, M. Oceanic minerals: Their origin, nature of their environment, and significance. *Proc. Natl. Acad. Sci. USA* **1999**, *96*, 3380–3387. [CrossRef] [PubMed]

46. Bainbridge, Z.; Wolanski, E.; Alvarez-Romero, J.G.; Lewis, S.E.; Brodie, J.E. Fine sediment and nutrient dynamics related to particle size and floc formation in a Burdekin River flood plume, Australia. *Mar. Pollut. Bull.* **2012**, *65*, 236–248. [CrossRef] [PubMed]

47. Hinds, W. *Aerosol Technology: Properties, Behavior, and Measurement of Airborne Particles*, 2nd ed.; John Wiley: New York, NY, USA, 1999.

48. Fennessy, M.; Dyer, K.; Huntley, D. INSSEV: An instrument to measure the size and settling velocity of flocs in situ. *Mar. Geol.* **1994**, *117*, 107–117. [CrossRef]

49. Vos, P.; De Boer, P.; Misdorp, R. Sediment stabilization by benthic diatoms in intertidal sandy shoals: Qualitative and quantitative observations. In *Tide-Influenced Sedimentary Environments and Facies*; D. Reidel Publishing: Dordrecht, The Netherlands, 1988; pp. 511–526.

50. Van der Lee, W.T.B. Temporal variation of floc size and settling velocity in the Dollard estuary. *Cont. Shelf Res.* **2000**, *20*, 1495–1511. [CrossRef]

51. Maerz, J.; Hofmeister, R.; van der Lee, E.M.; Grawe, U.; Riethmuller, R.; Wirtz, K.W. Maximum sinking velocities of suspended particulate matter in a coastal transition zone. *Biogeosciences* **2016**, *13*, 4863–4876. [CrossRef]

52. Van der Hout, C.M.; Wittbaard, R.; Bergman, M.J.M.; Duineveld, G.C.A.; Rozemeijer, M.J.C. The dynamics of suspended particulate matter (SPM) and chlorophyll-a from intratidal to annual time scales in a coastal turbidity maximum. *J. Sea Res.* **2017**. [CrossRef]

53. Khelifa, A.; Hills, P.S. Models for effective density and settling velocity of flocs. *J. Hydraul. Res.* **2006**, *44*, 390–401. [CrossRef]

54. Maggi, F. Variable fractal dimension: A major control for floc structure and flocculation kinematics of suspended cohesive sediment. *J. Geophys. Res. Oceans* **2007**, *112*, C07012. [CrossRef]

55. Van der Lee, W.T.B. Parameters affecting mud floc size on a seasonal time scale: The impact of a phytoplankton bloom in the Dollard estuary, The Netherlands. In *Coastal and Estuarine Fine Sediment Transport Processes*; McAnally, W.H., Mehta, A.J., Eds.; Elsevier: Amsterdam, The Netherlands, 2001; Volume 3, pp. 403–421.

56. Furukawa, Y.; Reed, A.H.; Zhang, G. Effect of organic matter on estuarine flocculation: A laboratory study using montmorillonite, humic acid, xanthan gum, guar gum and natural estuarine flocs. *Geochem. Trans.* **2014**, *15*, 1–9. [CrossRef] [PubMed]

57. Lee, B.J.; Hur, J.; Toorman, E. Seasonal Variation in Flocculation Potential of River Water: Roles of the Organic Matter Pool. *Water* **2017**, *9*, 335. [CrossRef]